E-ISSN 2586-9027
Homepage : https://tci-thaijo.org/index.php/SciTechAsia Science & Technology Asia
Vol.30 No.3 July - September 2025 Page: [78-86]
Original research article

A Robust Graph-based Method with Junction Detection and Angle Pruning for Longest Continuous Non-branching Vessel Segmentation in OCTA Images

Napat Tatiyakaroonwong, Haseeb Ali, Pakinee Aimmanee*

Sirindhorn International Institute of Technology, Thammasat University, Pathum Thani 12120, Thailand

Received 15 June 2025; Received in revised form 1 August 2025
Accepted 18 August 2025; Available online 30 September 2025

ABSTRACT

Optical coherence tomography angiography (OCTA) is a powerful imaging technique for non- invasively visualizing retinal blood flow at high resolution. Accurate vessel segmentation from OCTA images is essential for diagnosing and monitoring retinal diseases. However, segmentation remains challenging due to the complexity of the vessel network, including sharp turns, varying vessel widths, and frequent junctions. Additionally, denoising OCTA images without losing fine vessel structures further complicates the process. This study proposes an enhanced graph traversal method for OCTA vessel segmentation. Incorporating angular-threshold-based pruning and improved junction handling to address common challenges with a comprehensive preprocessing pipeline to denoise the OCTA image while preserving vessel integrity. It also gives a comparative analysis against a baseline graph traversal technique, which extracts all vessel paths without pruning or junction refinement. This research aims to enhance the accuracy of extraction of longest biologically realistic continuous vessel segments from an OCTA image. To evaluate our method, we use a dataset of five OCTA images each comprising of approximately 175 vessel segments and 60 longest vessel strains. Evaluation metrics include false positive rates and qualitative visual comparisons. Visual analysis demonstrates that our pruning technique significantly improves segmentation quality, producing smoother, continuous and biologically valid vessels while reducing spurious branches. Our results yield an F1 score of 0.8488, showing a marked improvement over the baseline model.

Keywords: A graph-based method; Angle pruning; Junction detection; OCTA vessel segmentation

***Corresponding author:** pakinee@siit.tu.ac.th **doi:** 10.14456/scitechasia.2025.49

1. Introduction

Optical Coherence Tomography Angiography (OCTA) is an advanced non-invasive imaging technique that allows for high-resolution visualization of the microvasculature within biological tissues, particularly in the retina. Unlike conventional imaging modalities, such as fluorescein angiography, OCTA does not require the injection of contrast dyes, making it a safer and more convenient option for diagnosing and monitoring retinal diseases. By capturing volumetric scans, OCTA enables detailed assessment of vascular structures within different retinal layers, providing a comprehensive view of blood flow dynamics.

A critical step in analyzing OCTA images is retinal vessel segmentation, which facilitates quantitative assessment of vascular features such as vessel density, tortuosity, and bifurcation patterns. However, accurate and robust segmentation remains a significant challenge due to several inherent complexities in the OCTA images. First, the retinal vessel exhibits structural complexity, characterized by vessels of varying diameters, sharp angular turns, and frequent branching or junction points. These features make it difficult to extract continuous and biologically realistic vessel paths. Second, OCTA images often suffer from speckle noise [1], projection artifacts and uneven illumination, which can obscure fine vessel structures or introduce false positives. Effective vessel segmentation must therefore balance noise suppression with structure preservation, especially for finer vessels.

Numerous vessel segmentation techniques have been proposed in recent years. Classical image processing techniques primarily rely on edge detection, thresholding, and morphological operations to delineate vessels. Frangis' Vesselness filter [2], based on multiscale analysis of the Hessian matrix, remains a popular choice for enhancing tubular structures. It performs well for vessels of various sizes but requires robust postprocessing to yield a clean vessel segmentation. More recent approaches also include deep learning methods [3, 4] which learn directly from labeled data. Although these methods have shown impressive accuracy, they typically require large, annotated datasets and may struggle to generalize across devices or imaging conditions.

While a significant body of research has focused on segmentation of the vessel network, relatively little attention has been given to the extraction of continuous, biologically valid longest vessel paths from the segmented network. This information is crucial for applications such as tortuosity analysis which is vital for early detection of various retinal diseases. Furthermore, reconstruction of such paths accurately, requires careful handling of junction points, angular continuity and noise-induced discontinuities – often overlooked in standard segmentation pipelines.

In this work we bridge that gap by introducing an enhanced graph traversal framework with an effective preprocessing pipeline which preserves finer vessel segments while removing noise effectively. It also segments the vessels and reconstructs longest, biologically meaningful vessel trajectories within the network. By incorporating angular-threshold-based pruning and robust junction handling into a tailored graph construction process, our method prioritizes anatomical realism and connectivity. This leads to smoother, more continuous vessel paths.

2. Methodology

Fig. 1 depicts procedures used in the methodology. The detail of each step is provided in the next sub sections.

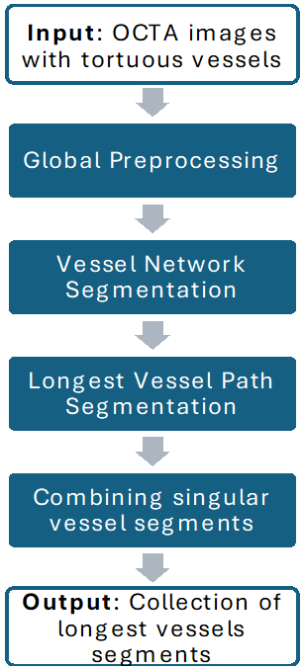

Fig. 1. Overall Framework of the proposed method.

2.1 Global preprocessing

Since colors were not essential for this work, the first step was to convert the images to grayscale. Afterwards, artifacts appearing as short horizontal and vertical lines during scanning, as well as text providing image information at the bottom right of the images, were removed to prevent accidental detection as vessels. We then performed Min-Max normalization, scaling the pixel intensities to a range of 0 to 255.

We enhanced clarity of the vessel edges by using the unsharp mask described by the work of Kim and Kim [5]. The process is as follows. For each point (x, y) in each channel, we applied the Gaussian blur algorithm, which is mathematically defined in Eq (2.1).

$$G(x, y, \sigma) = \frac{1}{2\pi\sigma^2} e^{\frac{-(x^2+y^2)}{2\sigma^2}}, \qquad (2.1)$$

where σ is the blur kernel. In our studies, we used $\sigma = 0.4$. The enhanced image Img_{enh} is achieved from the input image Img and the image after Gaussian blurring Img_{GB} with a sigma value of 1, as described in Eq. (2.2).

$$Img_{enh} = Img + 2 \times (Img - Img_{GB}). \qquad (2.2)$$

Next, we applied Contrast Limited Adaptive Histogram Equalization (CLAHE) filters with a clip limit of 1 and tile grid size of (8,8) for localized changes in contrast, to further enhance the contrast between the vessels and the background.

2.2 Vessel network segmentation

This step involves vessel separation into channels, vessel clarity enhancement for each channel, and the recombination of channels.

2.2.1 Image separation by vessel sizes

The enhanced image was split into three channels: small (S), medium (M) and large (L). These sizes were distinguished by using Hessian-based Frangi Vessel Filter [2] to each channel to detect the vessel structures and suppress non-vessel areas. For each channel, we used the ranges [1, 3], [4, 6], and [6, 10] for the S, M, and L channels, respectively.

2.2.2 Vessel clarity enhancement for each channel

We improved the contrast of each channel by reapplying CLAHE with clip limits of 4.0, 2.0, and 0.1 on the tile grid sizes of 4×4, 16×16, and 8×8 and filtered

out small objects of sizes 25, 50, and 70 pixels for the S, M, and L channels, respectively.

2.2.3 Constructing vessel networks from separate channels

We combined the cleaned preprocessed vessel networks from the three channels by pixelwise adding normalized vessel images from the channels together. We then binarized the images using Otsu's Thresholding method [6], and removed small objects of size smaller than 150 pixels. Then, we applied morphological closing and dilation [7] operations using kernel sizes of 3 and 2, respectively to fill the gaps between the continuous vessels that might have been introduced during the preprocessing. The images illustrating these processes are shown in Fig. 2.

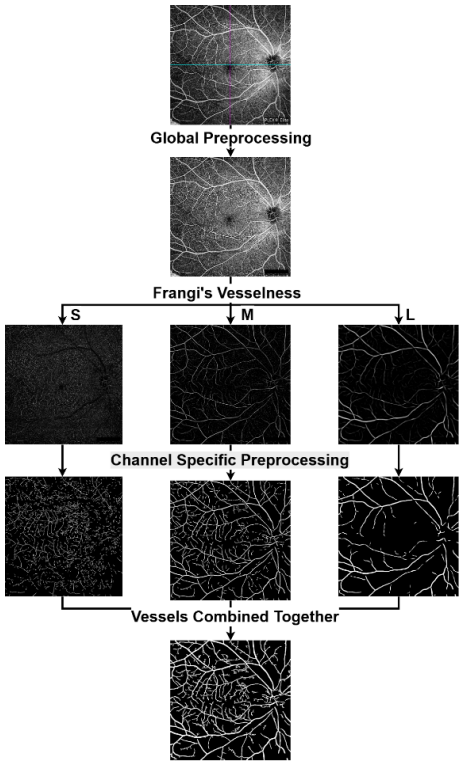

Fig. 2. Preprocessing pipeline.

2.3 Longest vessel path segmentation

The procedures in this step are depicted in Fig. 3, and details are summarized in the following subsections.

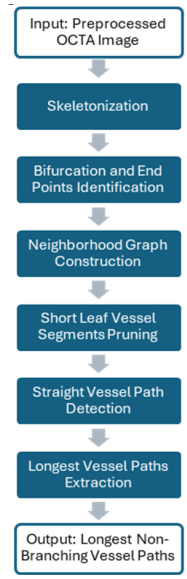

Fig. 3. Processes in the longest vessel path segmentation.

2.3.1 Skeletonization

In the analysis of vessel network topology, skeletonization serves to simplify the structural complexity while preserving the essential topological features of the network. In this study, a thinning algorithm [8] is applied to the preprocessed image to reduce the vessel structures to their centerlines, helping the identification of critical points required for further analysis.

2.3.2 Identifying bifurcation and end points

Bifurcation points and end points are key topological features that play a crucial role in constructing a neighborhood graph for traversal. To identify these points, the neighboring degree (*nbd*) of each point on the skeleton is computed. A *nbd* of a point p is defined as the number of adjacent vessel pixels in a nine-point grid centered at p.

A point is classified as a bifurcation if it exceeds two, and as an end point if its *nbd* is equal to one.

2.3.3 Constructing neighborhood graph

Bifurcation and end points are used as nodes for the neighborhood graph (NBG) to form a vessel network. The depth-first-search algorithm [9] is used to construct an NBG. The pseudo algorithm makeNBG depicts the processes.

Input: A skeleton image SK
Algorithm makeNBG(SK)
NBG is set to an empty graph
for each node s in SK
    subgraph = DFS(s, SK)
    NBG = merge(NBG, subgraph)
end
Output: NBG

The algorithm requires the following functions detailed below.

DFS(s, SK) takes the node s and the skeleton image as inputs, it returns a graph, which is a subgraph of SK, obtained from the depth-first-search algorithm starting at node s. merge(G1, G2): takes two graphs G1 and G2 as inputs and returns the union of the two graphs.

2.3.4 Pruning short leaf vessel segments

Leaf vessel segments (LVS) are segments with one end point and one bifurcation point. Short LVS typically contribute minimally to the resulting vessel paths and add unnecessary complexity to the analysis. Therefore, we pruned LVS with lengths below a specified threshold. In this work, the size threshold was set to 25 pixels.

2.3.5 Straight vessel path detection

In this study, the non-branching vessel paths (NBVP) are of our interest. The NBVP is defined as a sequence of continuous vessel segments of which the angle between two adjacent segments is more than 135 degrees. We specifically consider only paths longer than 50 pixels to reduce considered cases and improve running time. The fixed degree and path length was chosen based on our observation.

In addition, if a pair of NBVPs have a pixel difference of less than 8 pixels, they are considered the same NBVP, and the one with the shorter pixel will be kept. Fig. 4 depicts examples of NBVP and non-NBVP cases.

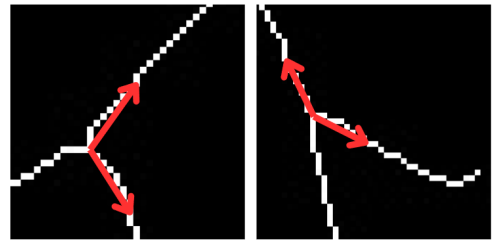

Fig. 4. Illustration of NBVP and non-NBVP cases.

It is important to note that the vessels are usually curvy and wavy, so we cannot compute the angle directly from them. Instead, an angle between two adjacent vessel segments A and B is defined at their common point in Eq. (2.3).

Let c be a common point of A and B, a be a point on A that is the 10th nearest to c, and b be a point on B that is the 10th nearest to c. The notations $\overrightarrow{ca}$ and $\overrightarrow{cb}$ denotes vectors from c to a and c to b, respectively.

$$angle(A,B) = \cos^{-1}\left(\frac{\overrightarrow{ca}}{\|\overrightarrow{ca}\|}\cdot\frac{\overrightarrow{cb}}{\|\overrightarrow{cb}\|}\right). \tag{2.3}$$

It is worth noting that the fixed distance of 10 nearest to the common point was selected empirically.

The algorithm findNBVP depicts how the vessel segments get added to a path NBVP starting at node x. It excludes already-visited vessel segments. In addition, it ensures that the last added vessel segment is not too short to be included in the path to save some computational costs. Segments are considered too short if their length is smaller than 8 pixels. We apply this algorithm to all nodes in NBG. This step is shown in the algorithm findNBVPs.

Input:
    A neighborhood graph NBG
    A set of vessel segments SS
Algorithm findNBVPS(NBG, SS)
NBVPS is set to an empty set
for each node s in NBG
    paths = findNBVP(NBG, SS, s)
    NBVPs = NBVP ⋃ paths
end
Output: NBVPs

Algorithm findNBVPS requires a recursive algorithm findNBVP defined below.

Input:
    NBG is a neighborhood graph
    SS is a set of vessel segments
    x is a starting node
Algorithm findNBVP(NBG, SS, x)
P is initialized to set of path segments containing node x
temp =
for each pair of p∈P and s∈SS
    if isValid(p, s) == true
      = append(p, s)
    endif
    temp = temp ⋃
end for
if temp is not empty
    P = P ⋃ temp
    findNBVP(NBG, SS, x)
Output: P

Remark: U is the set union operator. The algorithm requires the following functions detailed below. isValid(p, s): input a path p and a vessel segment s. It returns true if s has more than 8 pixels and *p* and *s* have a point in common, and the angle between the last segment of *p* and the segment *s* is greater than 135 degrees, or else return false. append(p, s): append the vessel segment s to the path p.

2.3.6 Longest vessel paths extraction

The valid vessel path set obtained from the previous section comprises all possible combinations of valid vessel paths. We then iterate through the valid vessel path set and remove any path that is a continuous subsequence of another path within the set. This process results in a set of longest unique valid vessel paths.

3. Experiments

3.1 Tested images

869 segments of vessels collected from five OCTA images provided by Thammasat University Hospital were used in this study. The original images were fovea-centered with dimension 12 by 12 mm. Each image was cropped to square patch of dimension 512 by 512 pixels. For ground truth, experts manually labelled the longest non-branching vessel paths.

3.2 Evaluation schemes

To quantitatively assess the performance of our vessel extraction methods, we employed three commonly used evaluation metrics: precision, recall and F1-score. These metrics are particularly well-suited for tasks involving sparse structures such as retinal vessel segmentation, where

the goal is to accurately identify continuous vessel paths within a large background region. The ground truth image, which features the longest continuous non-branching vessels labeled by humans, was compared to the algorithm-generated images across all endpoints. The evaluation was performed on a pixel-by-pixel basis.

These metrics are provided in Eqs. (3.1)-(3.3).

$$Precision = \frac{t_p}{t_p + f_p}, \tag{3.1}$$

$$Recall = \frac{t_p}{t_p + f_n}, \tag{3.2}$$

$$F1 - score = 2 \times \frac{Precision \times Recall}{Precision + Recall}. \tag{3.3}$$

where t_p stands for true positive and f_p for false positive, f_n stands for false negative true positive and t_n stands for true negative.

4. Results and Discussion

To evaluate the effectiveness of our proposed graph-based method, we conducted experiments on a set of five fovea-centered images as detailed in Section 3.1. The performance of our model was compared to a modified depth-first search (modified DFS) algorithm, which compares all vessel paths from one starting point without backtracking to finding the longest possible path. Fig. 5 compares the results from the two methods at a selected endpoint, indicated by a yellow circle.

We intentionally include only one endpoint in this illustration to maintain clarity and avoid cluttering the solutions. As shown in Fig. 5(c), the DFS-based method selects the longest vessel path, regardless of branches. In contrast, the proposed method focuses solely on straight or nearly straight vessels in the path, so it yielded the excellent results.

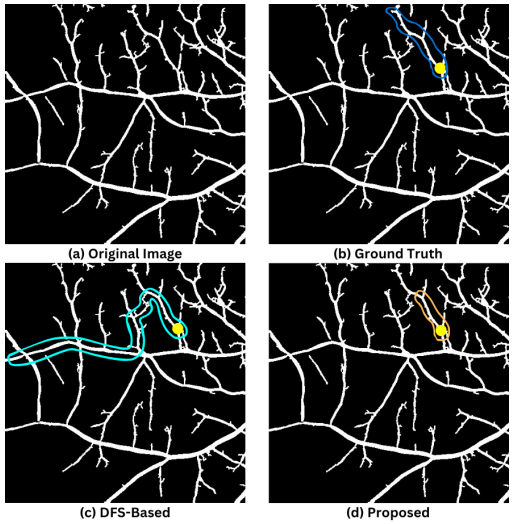

Fig. 5. Comparison of the baseline model and our method on the longest continuous non-branching vessel strains from one selected endpoint.

Table 1 presents precision, recall, F1-measure of the modified DFS and the proposed method.

Table 1. Performance comparison of our proposed method vs. the modified DFS method in percentage (%). The highest value in each evaluation is bold.

Method	Precision	Recall	F1-Score
Modified DFS	22.62	66.70	32.74
Proposed	**85.76**	**84.03**	**84.88**

As shown in Table 1, the proposed method significantly outperformed the baseline across all evaluation metrics, particularly in precision. The most notable improvement in precision is attributed to our advanced algorithm design, which utilizes angles to exclude vessels that branch off from the main path. In contrast, the modified DFS is hindered by the inclusion of irrelevant branch paths, leading to lower precision and, consequently, a reduced F1-score. The inaccuracy arises from incorrectly selected vessel segments, as the an-

gle was calculated based on representative points from two vessels. A very curvy vessel can lead the algorithm to make decisions about including or excluding it from the path that differs from what is appropriate. Another cause of the imperfect result is the angle threshold of 135 degrees. Some vessel angles slightly smaller than this threshold may be excluded rather than included.

5. Conclusion

In this study, we presented a robust graph-based method for extracting the longest continuous non-branching vessel segments from OCTA images. Our approach integrates a comprehensive preprocessing pipeline with angular threshold-based pruning and junction-aware graph traversal to address key challenges in retinal vessel segmentation – namely the presence of noise, frequent bifurcations, and complex vessel geometries.

Unlike conventional segmentation pipelines that focus primarily on binary vessel maps or pixel-wise classification, our method emphasizes the continuity and anatomical plausibility of the extracted vessel paths. By carefully handling bifurcation points and imposing angular constraints, we were able to significantly reduce spurious branches and preserve biologically realistic vessel trajectories.

We also comparatively analyzed our method against a baseline graph traversal algorithm, which confirmed the superiority of our method to the conventional approaches, in producing more realistic vessel segments – achieving an F1 score of 0.8488 compared to 0.3274 achieved by the baseline method.

Our method shows strong potential for downstream clinical applications such as tortuosity analysis further leading to early diagnosis of various retinal-related diseases. Future work may include enhancing the pre-processing pipeline, particularly in preserving faint or low-contrast vessels that are occasionally missed, leading to discontinuities. Additionally, refining the vessel pruning algorithm using more advanced policies could further improve accuracy and robustness.

Acknowledgements

The authors would like to thank the Thailand Science Research and Innovation (grant ID TUFF 48/2568) for their financial support for this study.

References

[1] Ma Y, Chen X, Zhu W, Cheng X, Xiang D, Shi F. Speckle noise reduction in optical coherence tomography images based on edge-sensitive cGAN. Biomed Opt Express. 2018 Oct 2;9(11).

[2] Frangi AF, Niessen WJ, Vincken KL, Viergever MA. Multiscale vessel enhancement filtering. Lecture Notes in Computer Science. 1998.

[3] Tan X, Chen X, Meng Q, Shi F, Xiang D, Chen Z, et al. OCT2Former: A retinal OCT-angiography vessel segmentation transformer. Comput Methods Programs Biomed. 2023 May 1;233.

[4] Ning H, Wang C, Chen X, Li S. An Accurate and Efficient Neural Network for OCTA Vessel Segmentation and a New Dataset. 2023 Sep 18.

[5] Kim J-y, Kim J-h. Design of Unsharp Mask Filter based on Retinex Theory for Image Enhancement. J Multimedia Inf Syst. 2017;4(2).

[6] Otsu N. A Threshold Selection Method from Gray-Level Histograms. IEEE Trans Syst Man Cybern. 1979;9(1):62-6.

[7] Serra J, Soille P. Mathematical Morphology and Its Applications to Image Processing. Dordrecht: Springer; 1994.

[8] Lee TC, Kashyap RL, Chu CN. Building skeleton models via 3-D medial surface/axis thinning algorithms. Comput Vis Graph Image Process. 1994;56(6):462-78.

[9] Tarjan R. Depth-First Search and Linear Graph Algorithms. SIAM J Comput. 2006 Jul 13;1(2).